

Chinese Chemical Society | Xiamen University

**Journal of Electrochemistry**

---

Online First

---

9-25-2023

## **Micropatterning and Functionalization of Single Layer Graphene: Tuning Its Electron Transport Properties**

Miaomiao Cui

Lianhuan Han

Lanping Zeng

Jiayao Guo

Weiyong Song

Chuan Liu

Yuanfei Wu

Shiyi Luo

Yunhua Liu

Dongping Zhan

—

# Micropatterning and Functionalization of Single Layer Graphene: Tuning Its Electron Transport Properties

Miaomiao Cui,<sup>a</sup> Lianhuan Han,<sup>a,b\*</sup> Lanping Zeng,<sup>a</sup> Jiayao Guo,<sup>a</sup> Weiying Song,<sup>a</sup> Chuan Liu,<sup>a</sup> Yuanfei Wu,<sup>a</sup> Shiyi Luo,<sup>a</sup> Yunhua Liu,<sup>c\*</sup> Dongping Zhan<sup>a\*</sup>

<sup>a</sup> Department of Chemistry, College of Chemistry and Chemical Engineering; State Key Laboratory of Physical Chemistry of Solid Surfaces (PCOSS); Engineering Research Center of Electrochemical Technologies of Ministry of Education; Xiamen University; Xiamen 361005, China.  
E-mail: dpzhan@xmu.edu.cn

<sup>b</sup> Department of Mechanical and Electrical Engineering, Pen-Tung Sah Institute of Micro-Nano Science and Technology, Xiamen University; Xiamen 361005, China.  
E-mail: hanlianhuan@xmu.edu.cn

<sup>c</sup> National CAD Support Software Engineering Research Center Huazhong University of Science and Technology, Wuhan 430074, China.  
E-mail: liuyh@mail.hust.edu.cn

**Keywords:** Graphene patterning, Electron transport, Electrochemical bromination, Photolithography, All graphene device

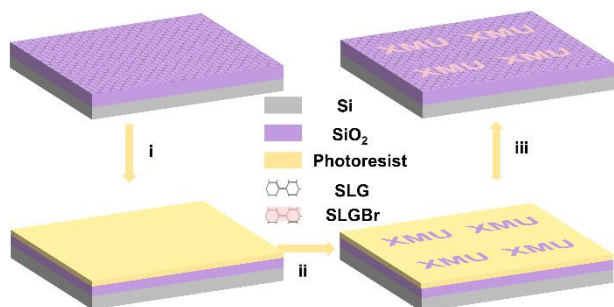
**Abstract:** As a promising 2D material, graphene exhibits excellent physical properties including single-atom-scale thickness and remarkably high charge carrier mobility. However, its semi-metallic nature with a zero bandgap poses challenges for its application in high-performance field-effect transistors (FETs). In order to overcome these limitations, various approaches have been explored to modulate graphene's bandgap, including nanoscale confinement, external field induction, doping, and chemical micropatterning. Nevertheless, the stability and controllability still need to be improved. In this study, we propose a feasible method that combines electrochemical bromination and photolithography to precisely tune the electron transport properties of single layer graphene (SLG). Through this method, we successfully fabricated various brominated SLG (SLGBr) micropatterns with high accuracy. Further investigation revealed that the electron transport properties of SLG can be conveniently tuned by controlling the degree of bromination. The SLGBr exhibited a resistance, and have a decreasing conductance with the bromination degree increasing. When the bromination degree increased to a critical value, the SLGBr demonstrated semiconducting characteristics. This research offers a prospective route for the fabrication of graphene-based devices, providing potential applications in the realm of microelectronics.

Graphene has been considered as the most prospective material because of its excellent properties, including single-atom-scale thickness<sup>[1]</sup>, extremely high charge carrier mobility<sup>[2]</sup>, superior optical transparency<sup>[3]</sup>, high thermal conductivity<sup>[4]</sup>, etc.. Recently, the mass production of high-quality single layer graphene (SLG) at wafer scale makes it qualified in various possible applications such as micro/nano-electronics, sensors and actuators, microelectromechanical system (MEMS), etc.<sup>[5-7]</sup>. To this, the localized micropatterning and functionalization of SLG at wafer scale is crucial in order to tune the physical and chemical properties, e.g., band gap, electron conductivity, transmittance, wettability, etc., and to fulfil the requirements of various industrial domains<sup>[8]</sup>.

Great efforts have been made to fabricate SLG patterns. Physical methods can be classified into top-down and bottom-up categories<sup>[9]</sup>. The top-down methods are to remove the carbon atoms from pristine SLG wafer by the energy-beam techniques including the focused laser beam, electron beam, plasma beam, reactive ion beam, etc.<sup>[10]</sup>. The top-down methods can be realized by either direct writing or template forming combined with various lithography techniques. The bottom-up methods are to synthesize specially sized SLG on the patterned catalysts such as copper, nickel, platinum, gold, etc.<sup>[11-13]</sup>. The most advantage of physical methods lies that the crystalline structure of SLG are not destroyed. Consequently, the intrinsic properties of SLG are kept very well. Nevertheless, the physical properties of SLG, e.g., the band gap, can be regulated by the external physical field<sup>[14]</sup>. However, when the external physical field were dismissed, the band gap of SLG would go back to zero.

Comparing physic methods, chemical micropatterning can change the crystalline structure and thus, change the physical and chemical properties of SLG<sup>[8]</sup>. Chemical adsorption<sup>[15]</sup> or doping<sup>[16]</sup> have been adopted to tune the SLG's properties by introducing the sp<sup>3</sup>-C defects. However, after thermal annealing, many of the functionalized SLG materials change back to be pristine due to the weak interaction between SLG and the adsorbates or dopants, e.g., van der Waals' force<sup>[17]</sup>, adsorption bond<sup>[18]</sup>, or even chemical bond<sup>[19]</sup>. To this, we developed an in-situ electrochemically induced radical addition reaction to functionalize SLG with high efficiency and stability<sup>[20, 21]</sup>. Here we report that the functionalized SLG micropatterns has tuneable electron transport properties, making SLG act as single-atomic-thickness resistor or rectifier, depending on the introduced sp<sup>3</sup>-C defects density.

The electrochemical micropatterning and functionalization procedures of SLG are depicted as in Scheme 1. First, a thin-layer viscosifier (HMDS) was spin-



**Scheme 1** Preparing processes of brominated SLG with patterns. (i) photoresist coating, (ii) Photolithography, (iii) electrochemical brominating.

1 coated on the SLG wafer to increase the adhesion between  
 2 SLG and photoresist. Second, a thin layer of photoresist  
 3 (AZ5214E) film was spin-coated on the substrate. Then, the  
 4 photoresist film was exposed by the laser-beam direct-  
 5 writing photolithography. Later on, the exposed photoresist  
 6 was removed by tetramethylammonium hydroxide for  
 7 several times and the aimed SLG micropattern array was  
 8 obtained. After that, the obtained SLG micropattern array  
 9 was immersed in an aqueous electrolyte containing 10 mM  
 10 KBr and 10 mM H<sub>2</sub>SO<sub>4</sub> to performed bromination addition  
 11 reaction by cyclic voltammetry in a potential range from -  
 12 0.75 to 1.2 V vs. Hg/Hg<sub>2</sub>SO<sub>4</sub> reference electrode with a  
 13 scan rate of 100 mV/s for certain cycles (See Figure S1).  
 14 Finally, the brominated SLG (SLGBr) micropatterns were  
 15 obtained after removing the photoresist protection layer by  
 16 rinsing with acetone and isopropanol.

17 As reported very recently by us, the functionalization  
 18 of SLG is realized by the bromination addition reaction<sup>[20]</sup>.  
 19 Because SLG is conductive enough to act as the working  
 20 electrode, bromide anions are oxidized to bromine radicals,  
 21 which can react with SLG to form SLGBr. When SLG  
 22 changes into SLGBr, the interfacial electrochemical reaction  
 23 activity will be decreased because the Faraday current  
 24 keeping decreasing with the potential scanning going on.  
 25 The SLGBr micropatterns "XMU", the acronym of Xiamen  
 26 University, were observed to have a different colour with  
 27 SLG by optical microscopy (Figure 1a). The corresponding  
 28 images of scanning electron microscopy (SEM) and  
 29 scanning Raman microscopy (SRM) were shown in Figure  
 30 1b and 1c. The clear boundaries between the SLG and  
 31 SLGBr were also observed, indicating the different  
 32 properties between them.

The Raman spectrum of the SLGBr region is much different from that of the SLG region (Figure 1d). The pristine SLG has a G-peak at near 1586 cm<sup>-1</sup> and a 2D peak at 2687 cm<sup>-1</sup>. The 2D-peak is sharp and symmetrical, and the peak intensity is about 4 times larger than that of G-peak, indicating that the pristine SLG has a perfect lattice structure<sup>[22]</sup>. After the functionalization by bromination addition reaction, the newly observed D-peak (~1350 cm<sup>-1</sup>) and D'-peak (~1620 cm<sup>-1</sup>) represents the sp<sup>3</sup>-C defects<sup>[23]</sup>, indicating that the symmetry of the lattice is changed due to the formation of C-Br bond. Furthermore, the G-peak blue-shifted to 1597 cm<sup>-1</sup> at the brominated region, and 2D peak blue-shifted to 2692 cm<sup>-1</sup>, predicting that SLGBr is p-type doping<sup>[24]</sup>, which is consistent with the strong electron absorption ability of bromine.

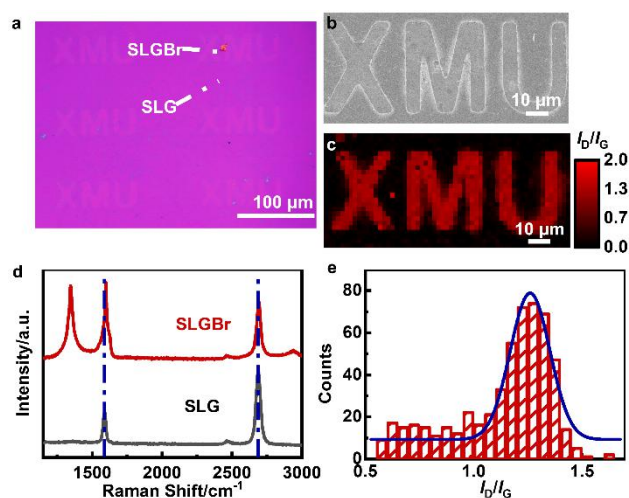


**Figure 1** The optical image (a) and SEM image (b) of patterned SLGBr with the "XMU" logo.(c) Raman  $I_D/I_G$  mapping of the patterned SLGBr. (d) The corresponding Raman spectra of pristine SLG and SLGBr. (e) Statistical  $I_D/I_G$  histograms from the mapping image of (c).

1 The intensity ratio ( $I_D/I_G$ ) is usually adopted to  
 2 characterize the defect density of graphene, that is, the  
 3 ratio of the  $sp^3$  to  $sp^2$  bonding character. A higher the  $I_D/I_G$   
 4 ratio means a higher defect density<sup>[25]</sup>. The statistical  
 5 analysis of SRM image gives a distribution of  $I_D/I_G$  ratio as  
 6 shown in Figure 1c. The  $I_D/I_G$  ratio in the “XMU” region is  
 7 much higher than that in the remaining region, which  
 8 indicates that photoresist micropattern can protect well the  
 9 underlying graphene and let the bromination addition  
 10 reaction selectively occur in the exposed area. The  
 11 statistical  $I_D/I_G$ -ratio histogram was employed to analyzed  
 12 the bromination degree of SLG. From Figure 1e,  $I_D/I_G$   
 13 ranged from 0.5 to 1.5 with a mid-value about 1.2,  
 14 suggesting that the bromination degree of SLGBr  
 15 micropattern was pretty uniform.

16 To demonstrate the versatility and reliability of the  
 17 method, SLGBr micropattern array such as square ring,  
 18 cross and an H- type Chinese knot were fabricated. The  
 19 optical microscopy images of the SLG micropatterns after  
 20 laser-beam direct-writing photolithography were shown in  
 21 Figure 2a-2c, and the relevant optical images of the SLGBr  
 22 micropatterns were shown in Figure. S2, indicating the clear  
 23 SLG/SLGBr boundaries. The relevant  $I_D/I_G$  distribution of  
 24 the SLGBr micropatterned SLG was characterized by the  
 25 SRM as shown in Figure 2d-2f, indicating the uniform  
 26 functionalization of bromination addition reaction.

27 We have demonstrated that the electron transport (i.e.,  
 28 electronic properties) and interfacial electron transfer (i.e.,  
 29 electrochemical properties) of functionalized SLG will change a  
 30 lot from the pristine SLG<sup>[20]</sup>. To investigate the electron transport  
 31 properties of SLGBr, we designed and fabricated the SLG-  
 32 SLGBr interdigitated electrodes with a pair of Cr/Au belts as the  
 33 current collectors (Scheme 2) to construct a field-effect transistor  
 34 (FET), where the SLG electrode acts as the drain, the SLGBr  
 35 acts as the source, and the Si/SiO<sub>2</sub> substrate acts as the gate. In  
 36 order to investigate the characteristics of the devices, SLG

electrodes and SLGBr electrodes were prepared simultaneously.  
 The SLG electrodes exhibit resistance characteristics and p  
 doping due to the residual photoresist (Figure S 3a-3b), while  
 the SLGBr electrodes with higher defect density showed  
 semiconducting characteristics (Figure S 3c-3d). Akin to  
 chemical functionalization, electrochemically induced  
 bromination addition introduced new  $sp^3$  C-Br bond to SLG.  
 Because of the asymmetric broken honeycomb structure, the  
 bandgap of SLGBr rises, and a semimetal–semiconductor  
 transition takes place in SLGBr.

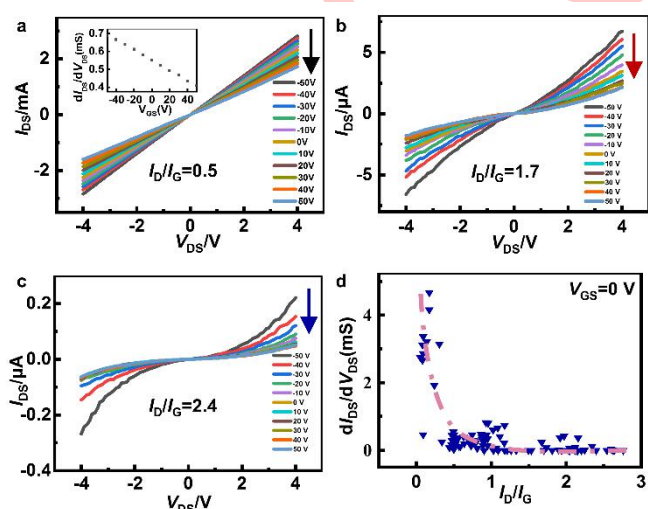


**Figure 3** (a-c) The  $I_{DS}$ - $V_{DS}$  curves of the SLGBr Interdigitated Electrode when  $I_D/I_G$  value is 0.5, 1.7 and 2.4, respectively. Inset: the slope of the  $I_{DS}$ - $V_{DS}$  curves changes with  $V_{GS}$ . (d) The statistic relationship curve between the bromination degree ( $I_D/I_G$ ) and the conductance ( $dI_{DS}/dV_{DS}$ ) at  $V_{GS} = 0$  V.

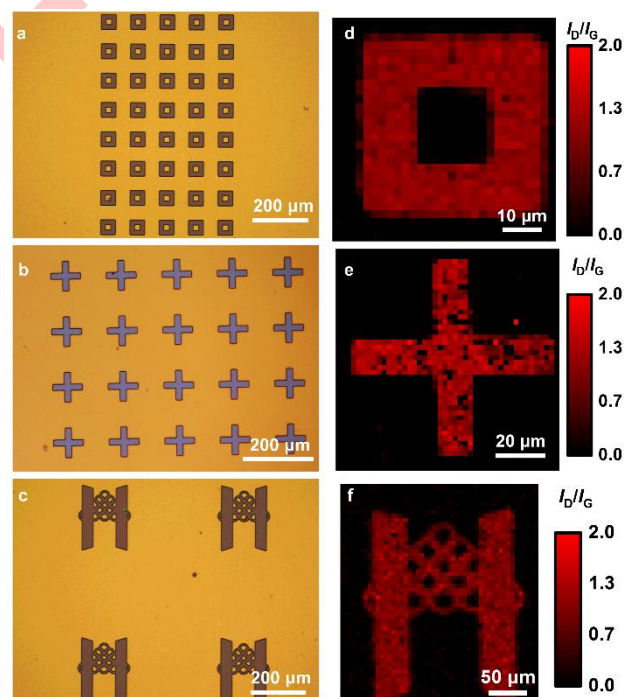
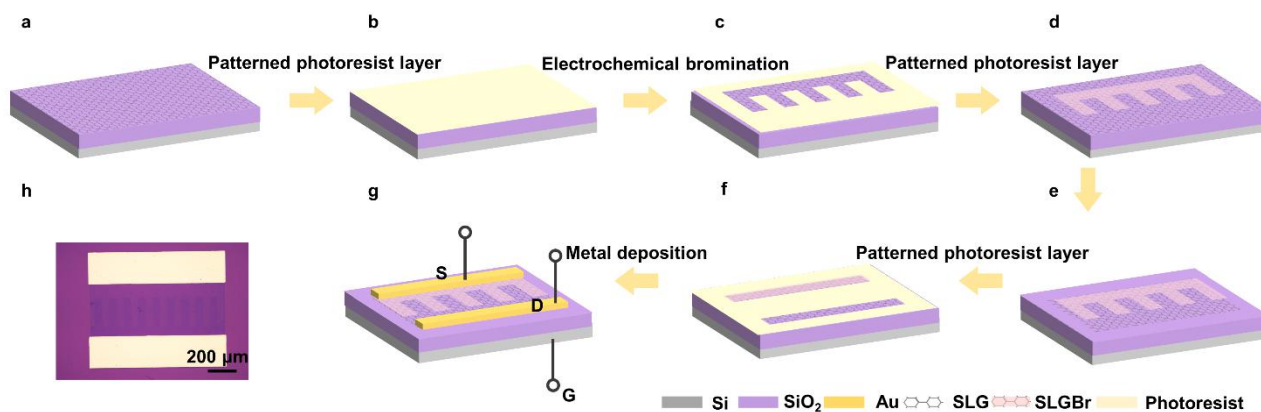


**Figure 2** (a-c) Optical images of SLG with photoresist patterns, including (a) square rings, (b) crosses and (c) H- type Chinese knot. (d-f) Corresponding Raman  $I_D/I_G$  mapping of the SLGBr patterns.





**Scheme 2** (a-g) Preparing processes of the graphene Interdigitated Electrodes with designed SLGBr patterns. (h) The optical image of a typical Interdigitated Electrode with patterned SLGBr.

1 Figure 3a-3c show the  $I_{DS}-V_{DS}$  curves of the SLGBr/SLG FET  
 2 with different bromination degree characterized by the statistical  
 3  $I_D/I_G$  mid-values from the SRM images of SLGBr. With the low  
 4 bromination degree ( $I_D/I_G$ : 0.5 in Figure 3a), the  $I_{DS}-V_{DS}$  curves  
 5 shows a typical electronic property of a resistor. The  
 6 conductance, i.e., the slope of the  $I_{DS}-V_{DS}$  curves changes  
 7 linearly with  $V_{GS}$  in a potential region [-50 V, +50 V], shown as  
 8 the insert of Figure 3a. The voltage-sensitive feature  
 9 demonstrates the potential application of SLG into micro-varistor.  
 10 With the higher bromination degree ( $I_D/I_G$ : 1.7 in Figure 3b or 2.4  
 11 in Figure 3c), the  $I_{DS}-V_{DS}$  curves were obviously different from  
 12 those in Figure 3a, presenting the characteristics of current  
 13 rectification. The results show that the SLGBr will be changed  
 14 into a semiconductor if the bromination degree becomes  
 15 higher<sup>[20, 26]</sup>. This result is similar to our previous study, but due  
 16 to the low degree of bromination, the semiconductor  
 17 characteristics are less significant than before<sup>[23]</sup>. We performed  
 18 the electronic measurements of the FETs with different  
 19 bromination degree and different  $V_{GS}$  bias, and the statistic  
 20 relationship between the conductance ( $dI_{DS}/dV_{DS}$ ) and the  
 21 bromination degree ( $I_D/I_G$ ) is shown in Figure 3d. The critical  $I_D/I_G$   
 22 value between conductor and semiconductor can be estimated  
 23 as 0.6. The mechanisms of the change of electron transport  
 24 properties needs to be further studied in future.

25 In conclusion, laser beam direct-writing photolithography and  
 26 electrochemically induced bromination addition reaction were  
 27 adopted for the micropatterning and functionalization of SLG.  
 28 We found that the brominating functionalization can tune the  
 29 electron transport properties of SLG by controlling its  
 30 bromination degree. The conductance of SLGBr keeps  
 31 decreasing at low bromination degree. After a critical value,  
 32 SLGBr will become a semiconductor. This work demonstrates  
 33 the possibility for the fabrication of ultrathin microelectronic  
 34 devices by SLG.

## 35 Supporting Information

36 Supporting information for this article is given via a link at the  
 37 end of the document. ((Please delete this text if not appropriate.))

## 38 Acknowledgements

The financial support by the National Natural Science Foundation of China (21827802, 22202166, 22132003, 22021001) and the 111 Project (B08027, B17027) are appreciated. We thank Tan Kah Kee Innovation Laboratory for providing characterization services.

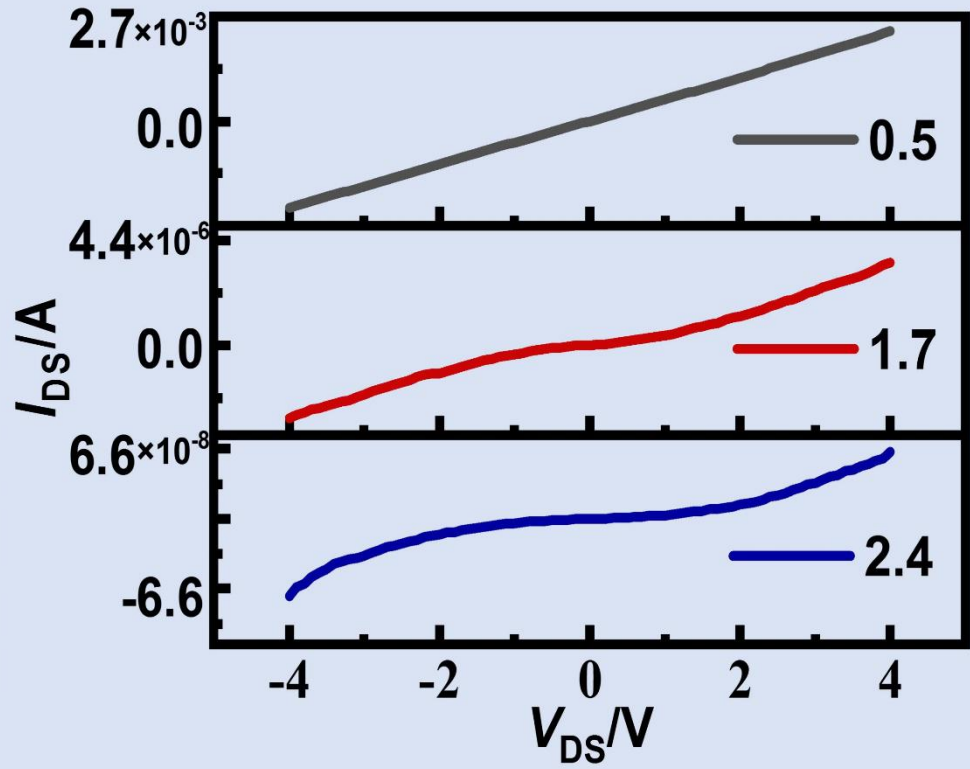
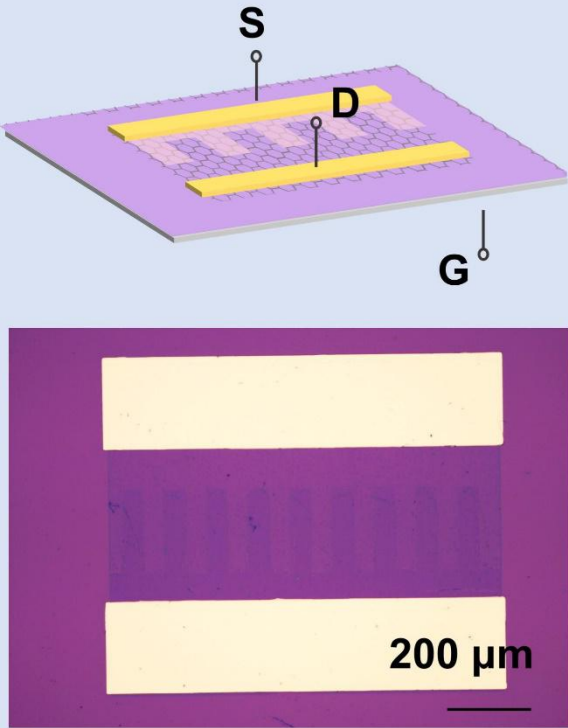
## References

- [1] Kaplan A, Yuan Z, Benck JD, Govind Rajan A, Chu XS, Wang QH, Strano MS. Current and Future Directions in Electron Transfer Chemistry of Graphene[J]. Chem. Soc. Rev.,2017, 46(15): 4530-4571.
- [2] Morozov SV, Novoselov KS, Katsnelson MI, Schedin F, Elias DC, Jaszczak JA, Geim AK. Giant Intrinsic Carrier Mobilities in Graphene and Its Bilayer[J]. Phys. Rev. Lett.,2008, 100(1): 016602.
- [3] Nair RR, Blake P, Grigorenko AN, Novoselov KS, Booth TJ, Stauber T, Peres NM, Geim AK. Fine Structure Constant Defines Visual Transparency of Graphene[J]. Science,2008, 320(5881): 1308.
- [4] Nan HY, Ni ZH, Wang J, Zafar Z, Shi ZX, Wang YY. The Thermal Stability of Graphene in Air Investigated by Raman Spectroscopy[J]. Journal of Raman Spectroscopy,2013, 44(7): 1018-1021.
- [5] He Q, Wu S, Yin Z, Zhang H. Graphene-Based Electronic Sensors[J]. Chem. Sci.,2012, 3(6): 1764-1772.
- [6] Biro LP, Nemes-Incze P, Lambin P. Graphene: Nanoscale Processing and Recent Applications[J]. Nanoscale,2012, 4(6): 1824-1839.
- [7] Schwierz F, Pezoldt J, Granzner R. Two-Dimensional Materials and Their Prospects in Transistor Electronics[J]. Nanoscale,2015, 7(18): 8261-8283.
- [8] Wei T, Bao L, Hauke F, Hirsch A. Recent Advances in Graphene Patterning[J]. Chempluschem,2020, 85(8): 1655-1668.
- [9] Wei T, Hauke F, Hirsch A. Evolution of Graphene Patterning: From Dimension Regulation to Molecular Engineering[J]. Adv. Mater.,2021, 33(45): 2104060.
- [10] Zheng YQ, Wang H, Hou SF, Xia DY. Lithographically Defined Graphene Patterns[J]. Advanced Materials Technologies,2017, 2(5): 1600237
- [11] Park JU, Nam S, Lee MS, Lieber CM. Synthesis of Monolithic Graphene-Graphite Integrated Electronics[J]. Nat. Mater.,2011, 11(2): 120-125.
- [12] Choi J-K, Kwak J, Park S-D, Yun HD, Kim S-Y, Jung M, Kim SY, Park K, Kang S, Kim S-D, Park D-Y, Lee D-S, Hong S-K, Shin H-J, Kwon S-Y. Growth of Wrinkle-Free Graphene on Texture-Controlled Platinum Films and Thermal-Assisted Transfer of Large-Scale Patterned Graphene[J]. ACS Nano,2015, 9(1): 679-686.
- [13] Zhou X, Qi Y, Shi J, Niu J, Liu M, Zhang G, Li Q, Zhang Z, Hong M, Ji Q, Zhang Y, Liu Z, Wu X, Zhang Y. Modulating the Electronic Properties of

- 1 Monolayer Graphene Using a Periodic Quasi-One-Dimensional Potential  
2 Generated by Hex-Reconstructed Au(001)[J]. ACS Nano,2016, 10(8):  
3 7550-7557.
- 4 [14] Zhang Y, Tang TT, Girit C, Hao Z, Martin MC, Zettl A, Crommie MF, Shen  
5 YR, Wang F. Direct Observation of a Widely Tunable Bandgap in Bilayer  
6 Graphene[J]. Nature,2009, 459(7248): 820-823.
- 7 [15] Balog R, Jørgensen B, Nilsson L, Andersen M, Rienks E, Bianchi M,  
8 Fanetti M, Lægsgaard E, Baraldi A, Lizzit S, Sljivancanin Z, Besenbacher F,  
9 Hammer B, Pedersen TG, Hofmann P, Hornekær L. Bandgap Opening in  
10 Graphene Induced by Patterned Hydrogen Adsorption[J]. Nat. Mater.,2010,  
11 9(4): 315-319.
- 12 [16] Wu J, Xie L, Li Y, Wang H, Ouyang Y, Guo J, Dai H. Controlled Chlorine  
13 Plasma Reaction for Noninvasive Graphene Doping[J]. J. Am. Chem.  
14 Soc.,2011, 133(49): 19668-19671.
- 15 [17] Yavari F, Kritzing C, Gaire C, Song L, Gulapalli H, Borca-Tasciuc T,  
16 Ajayan PM, Koratkar N. Tunable Bandgap in Graphene by the Controlled  
17 Adsorption of Water Molecules[J]. Small,2010, 6(22): 2535-2538.
- 18 [18] Elias DC, Nair RR, Mohiuddin TM, Morozov SV, Blake P, Halsall MP,  
19 Ferrari AC, Boukhvalov DW, Katsnelson MI, Geim AK, Novoselov KS.  
20 Control of Graphene's Properties by Reversible Hydrogenation: Evidence  
21 for Graphane[J]. Science,2009, 323(5914): 610-613.
- 22 [19] Wei T, Kohring M, Chen M, Yang S, Weber HB, Hauke F, Hirsch A. Highly  
23 Efficient and Reversible Covalent Patterning of Graphene: 2d-Management  
24 of Chemical Information[J]. Angew. Chem. Int. Ed. Engl.,2020, 59(14):  
25 5602-5606.
- 26 [20] Zeng L, Song W, Jin X, He Q, Han L, Wu Y-f, Lagrost C, Leroux Y, Hapiot  
27 P, Cao Y, Cheng J, Zhan D. Electrochemical Regulation of the Band Gap  
28 of Single Layer Graphene: From Semimetal to Semiconductor[J]. Chem.  
29 Sci.,2023.
- 30 [21] Chen DH, Lin Z, Sartin MM, Huang TX, Liu J, Zhang QG, Han LH, Li JF,  
31 Tian ZQ, Zhan DP. Photosynergetic Electrochemical Synthesis of  
32 Graphene Oxide[J]. J. Am. Chem. Soc.,2020, 142(14): 6516-6520.
- 33 [22] Zhong JH, Zhang J, Jin X, Liu JY, Li Q, Li MH, Cai W, Wu DY, Zhan D,  
34 Ren B. Quantitative Correlation between Defect Density and  
35 Heterogeneous Electron Transfer Rate of Single Layer Graphene[J]. J. Am.  
36 Chem. Soc.,2014, 136(47): 16609-16617.
- 37 [23] Ferrari AC, Basko DM. Raman Spectroscopy as a Versatile Tool for  
38 Studying the Properties of Graphene[J]. Nat. Nanotechnol.,2013, 8(4): 235-  
39 246.
- 40 [24] Li W, Li Y, Xu K. Facile, Electrochemical Chlorination of Graphene from  
41 an Aqueous NaCl Solution[J]. Nano Lett.,2021, 21(2): 1150-1155.
- 42 [25] Eckmann A, Felten A, Mishchenko A, Britnell L, Krupke R, Novoselov KS,  
43 Casiraghi C. Probing the Nature of Defects in Graphene by Raman  
44 Spectroscopy[J]. Nano Lett.,2012, 12(8): 3925-3930.
- 45 [26] Li B, Zhou L, Wu D, Peng HL, Yan K, Zhou Y, Liu ZF. Photochemical  
46 Chlorination of Graphene[J]. ACS Nano,2011, 5(7): 5957-5961.

47  
48

- 1
- 2 **Entry for the Table of Contents**



- 3
- 4
- 5
- 6
- 7
- 8
- 9

# 单层石墨烯微米尺度图案化和功能化：调控电子传输特性

崔苗苗<sup>a</sup>, 韩联欢<sup>a,b\*</sup>, 曾兰平<sup>a</sup>, 郭佳瑶<sup>a</sup>, 宋维英<sup>a</sup>, 刘川<sup>a</sup>, 吴元菲<sup>a</sup>, 罗世翊<sup>a</sup>, 刘云华<sup>c\*</sup>, 詹东平<sup>a\*</sup>

(<sup>a</sup>. 化学化工学院化学系;固体表面物理化学国家重点实验室, 电化学技术教育部工程研究中心, 厦门大学, 厦门 361005

<sup>b</sup> 厦门大学萨本栋微纳米科学与技术研究所机电工程系, 厦门大学, 厦门 361005

<sup>c</sup> 华中科技大学国家 CAD 支撑软件工程研究中心, 武汉 430074)

**摘要:** 石墨烯具有优异的物理特性, 如单原子厚度、极高的载流子迁移率等。然而, 其零带隙的半金属特性限制了题在高性能场效应晶体管中的应用。为此, 研究者们提出了石墨烯纳米化、外场诱导、掺杂以及化学图案化等策略, 以调控其带隙宽度。但是, 这些方法的可控性以及稳定性还需要进一步改善。在本研究中, 我们提出采用电化学溴化并结合光刻图案化调控单层石墨烯的电子传输特性。通过这种方法, 我们成功制备了图案化的溴化石墨烯 (SLGBr)。进一步研究表明单层石墨烯的电子传输性能可以通过溴化程度来调控。当溴化程度较小时, SLGBr 表现为电阻特性, 且其电导随溴化程度增加而减小; 当溴化程度增加到一定值时, SLGBr 表现为与半导体类似的特性。本研究将为全石墨烯器件的制备提供可行的技术路线, 拓展其在微电子领域的应用。

**关键词:** 石墨烯图案化; 电子传输; 电化学溴化; 光刻; 全石墨烯器件